Evidence for the $N'(1720)3/2^+$ Nucleon Resonance from Combined Studies of CLAS $\pi^+\pi^- p$ Photo- and Electroproduction Data

V.I. Mokeev[a,*], V.D. Burkert[a], D.S. Carman[a], L. Elouadrhiri[a], E. Golovatch[b], R.W. Gothe[c], K. Hicks[d], B.S. Ishkhanov[b], E.L. Isupov[b], K. Joo[e], N. Markov[a,e], E. Pasyuk[a], A. Trivedi[c]

[a] *Thomas Jefferson National Accelerator Facility, Newport News, Virginia 23606, USA*
[b] *Skobeltsyn Institute of Nuclear Physics and Physics Department, Lomonosov Moscow State University, 119234 Moscow, Russia*
[c] *University of South Carolina, Columbia, South Carolina 29208, USA*
[d] *Ohio University, Athens, Ohio 45701, USA*
[e] *University of Connecticut, Storrs, Connecticut 06269, USA*

Abstract

The analysis of the nine 1-fold differential cross sections for the $\gamma_{r,v}p \to \pi^+\pi^- p$ photo- and electroproduction reactions obtained with the CLAS detector at Jefferson Laboratory was carried out with the goal to establish the contributing resonances in the mass range from 1.6 GeV to 1.8 GeV. In order to describe the photo- and electroproduction data with Q^2-independent resonance masses and hadronic decay widths in the Q^2 range below 1.5 GeV^2, it was found that an $N'(1720)3/2^+$ state is required in addition to the already well-established nucleon resonances. This work demonstrates that the combined studies of $\pi^+\pi^- p$ photo- and electroproduction data are vital for the observation of this resonance. The contributions from the $N'(1720)3/2^+$ state and the already established $N(1720)3/2^+$ state with a mass of 1.745 GeV are well separated by their different hadronic decays to the $\pi\Delta$ and ρp final states and the different Q^2-evolution of their photo-/electroexcitation amplitudes. The $N'(1720)3/2^+$ state is the first recently established baryon resonance for which the results on the Q^2-evolution of the photo-/electrocouplings have become available. These results are important for the exploration of the nature of the "missing" baryon resonances.

Keywords: two pion production, resonance couplings, missing resonances
PACS: 11.55.Fv, 13.40.Gp, 13.60.Le, 14.20.Gk

1. Introduction

Studies of the N^* spectrum have been driven for a long time by the search for the so-called "missing" baryon states [1, 2, 3, 4, 5]. Different quark models predict many more excited states than those that have been observed in experiments [6, 7, 8]. These predictions rely on the approximate SU(6) spin-flavor symmetry demonstrated by the pattern of the observed nucleon resonances [9]. These model expectations are supported by the studies of the N^* spectrum from the QCD Lagrangian within Lattice-QCD (LQCD) [10], consistent with the independent results from continuum QCD approaches [11, 12]. In the early few μs expansion phase of the universe, the transition from a deconfined mixture of almost massless bare quarks and gauge gluons to a hadron gas of confined quarks and gluons with dynamically generated masses was mediated by the full spectrum of excited hadrons. This has been demonstrated in the studies of this phenomenon within LQCD and quark models [13]. Studies of the N^* spectrum, therefore, address the important open questions on the symmetry of the strong QCD dynamics underlying nucleon resonance generation and on the emergence of hadronic matter in the universe.

The data for exclusive meson photoproduction offer a promising avenue in the search for missing resonances [1, 2, 3, 4, 5] through their decays into final states other than the most explored πN channel. The missing resonances are expected to have substantial decays to the ηN, $K\Lambda$, $K\Sigma$, $\pi\pi N$, and $\pi\eta N$ final states accessible in photoproduction, where their photocouplings are expected to be comparable with those for the observed resonances [6, 7, 14]. Recently, several of the long-awaited missing resonances were discovered in a global multi-channel analysis of exclusive meson photoproduction data [15], for which the CLAS KY photoproduction data [16, 17, 18, 19] provided a decisive impact. Nine new nucleon resonances of three- or four-star status were included in the recent edition of the PDG [20]. This discovery is consistent with the expectation of SU(6) symmetry in the generation of the N^* spectrum. However, this symmetry also predicts many other resonances that have not yet been observed, making a continuation of the efforts on the missing resonance search an important avenue in hadron physics.

*Principal corresponding author
Email address: mokeev@jlab.org (V.I. Mokeev)

The CLAS data on exclusive meson electroproduction have extended the capabilities in the search for further missing resonances [21, 22, 23]. Both the πN and $\pi^+\pi^- p$ electroproduction data demonstrate an increase in the relative resonant contributions with increasing four-momentum transfer Q^2 [24, 25], making exclusive electroproduction also promising for the exploration of the N^* spectrum. A successful description of both the photo- and electroproduction data with Q^2-independent resonance masses, and total and partial hadronic decay widths, validates the existence of resonance states. In this paper, we present evidence for a new $N'(1720)3/2^+$ resonance that has been observed together with the known $N(1720)3/2^+$ state from combined studies of the CLAS $\pi^+\pi^- p$ photo- and electroproduction data [23, 26] for invariant masses W from 1.6 – 1.8 GeV in the range of photon virtualities $Q^2 < 1.5$ GeV^2. A global multi-channel analysis of exclusive meson photoproduction data [27] reports two close resonances with $J^P = 3/2^+$ spin-parity in the 1.7 – 1.8 GeV mass range. Also quark models [7, 8, 28] expect new low-lying baryon states with $J^P = 3/2^+$ in this mass interval.

2. Experimental Data and Analysis Tools

In the previous studies of CLAS $\pi^+\pi^- p$ electroproduction data off protons [23], two invariant mass distributions over $M_{\pi^+ p}$ and $M_{\pi^+\pi^-}$, and the π^- center-of-mass (CM) angular distributions were analyzed for W from 1.6 – 1.8 GeV and Q^2 from 0.5 – 1.5 GeV^2. A pronounced resonance structure at $W \approx 1.7$ GeV was observed in all three Q^2 bins covered by these data centered at 0.65 GeV^2, 0.95 GeV^2, and 1.3 GeV^2 (see Fig. 1). A successful description of these data was only achieved either with a much larger branching fraction for the $N(1720)3/2^+$ resonance decays to the $\pi\Delta$ final state in comparison with those from experiments with hadron probes or by implementing a new $N'(1720)3/2^+$ baryon state with parameters determined from the data fit. Both solutions offered an equally reasonable description of the limited previous CLAS $\pi^+\pi^- p$ electroproduction data set.

In the current analysis we unambiguously established the resonances contributing to $\pi^+\pi^- p$ photo- and electroproduction in the third resonance region. We have analyzed the data for this channel on the nine 1-fold differential cross sections and fully integrated cross sections over the final state kinematic variables sorted into nine 25-MeV-wide bins in W and four Q^2-bins at 0 GeV^2, 0.65 GeV^2, 0.95 GeV^2, and 1.30 GeV^2. The fully integrated cross sections and their description achieved within the the JLab-Moscow (JM) meson-baryon model [29, 30, 31] are shown in Fig. 1.

The production of the $\pi^+\pi^- p$ final state hadrons can be fully described by the 5-fold differential cross section over the invariant masses of the two pairs of the final state hadrons M_{ij}, M_{jk} $(i, j, k = \pi^+, \pi^-, p')$ and over the three angular variables shown in Fig. 2. After integration of the 5-fold differential cross section over the different sets of four variables, nine 1-fold differential cross sections were determined for:

a) Three invariant mass distributions: $\frac{d\sigma}{dM_{\pi^+ p'}}$, $\frac{d\sigma}{dM_{\pi^+\pi^-}}$, $\frac{d\sigma}{dM_{\pi^- p'}}$;
b) Three angular distributions over θ: $\frac{d\sigma}{d(-\cos\theta_{\pi^-})}$, $\frac{d\sigma}{d(-\cos\theta_{\pi^+})}$, $\frac{d\sigma}{d(-\cos\theta_{p'})}$;
c) Three angular distributions over α: $\frac{d\sigma}{d\alpha_{[\pi^- p][\pi^+ p']}}$, $\frac{d\sigma}{d\alpha_{[\pi^+ p][\pi^- p']}}$, $\frac{d\sigma}{d\alpha_{[p' p][\pi^+\pi^-]}}$.

The chosen nine 1-fold differential cross sections are the most suitable for the exploration of the nucleon resonances excited in the $\gamma_{r,v} + p$ s-channel with subsequent decays into the $\pi\Delta$ and ρp final states. The kinematic grid and the number of data points incorporated into the analysis are listed in Table 1. Each of the nine 1-fold differential cross sections, while computed from a common 5-fold differential cross section, offers complementary information that is essential to gain insight into the resonant contributions.

The data analysis is carried out within the JM model. This approach incorporates all essential mechanisms seen in the data that give rise to peaks in the invariant masses and the sharp dependencies in the angular distributions. Less pronounced mechanisms were established from the correlations between their contributions into the different 1-fold differential cross sections. The full $\gamma_{r,v} p \to \pi^+\pi^- p'$ amplitudes are described in the JM model as a superposition of the $\pi^-\Delta^{++}$, $\pi^+\Delta^0$, ρp, $\pi^+ D^0_{13}(1520)$, and $\pi^+ F^0_{15}(1685)$ sub-channels with subsequent decays of the unstable hadrons to the final state, and direct 2π production mechanisms, where the reaction does not go through the intermediate process of forming unstable hadrons. The JM model incorporates contributions from all well-established N^* states with observed decays into the $\pi\Delta$ and ρp final states listed in Refs. [26, 31]. For the resonant amplitudes, a unitarized Breit-Wigner ansatz is employed, which makes the resonant amplitudes consistent with restrictions imposed by a general unitarity condition [30].

The good description of the nine 1-fold differential $\pi^+\pi^- p$ photo- and electroproduction cross sections, achieved within the JM model for $W < 2.0$ GeV and in the Q^2-range up to 5.0 GeV^2, allows isolation of the resonant contributions [21, 26, 31] necessary for the extraction of the resonance parameters. The N^* photo-/electroexcitation amplitudes ($\gamma_{r,v} p N^*$ photo-/electrocouplings) were determined from analyses of the $\pi^+\pi^- p$ photo-/electroproduction data for the resonances in the mass range up to 2.0 GeV from the photoproduction data and up to 1.8 GeV from the electroproduction data. Consistent results on the electrocouplings of the $N(1440)1/2^+$ and $N(1520)3/2^-$ resonances in the Q^2-range from 0.2 GeV^2 to 5.0 GeV^2 from independent analyses of the dominant πN and $\pi^+\pi^- p$ electroproduction channels validates the extracted N^* parameters from the JM model. The photocouplings of most resonances in the

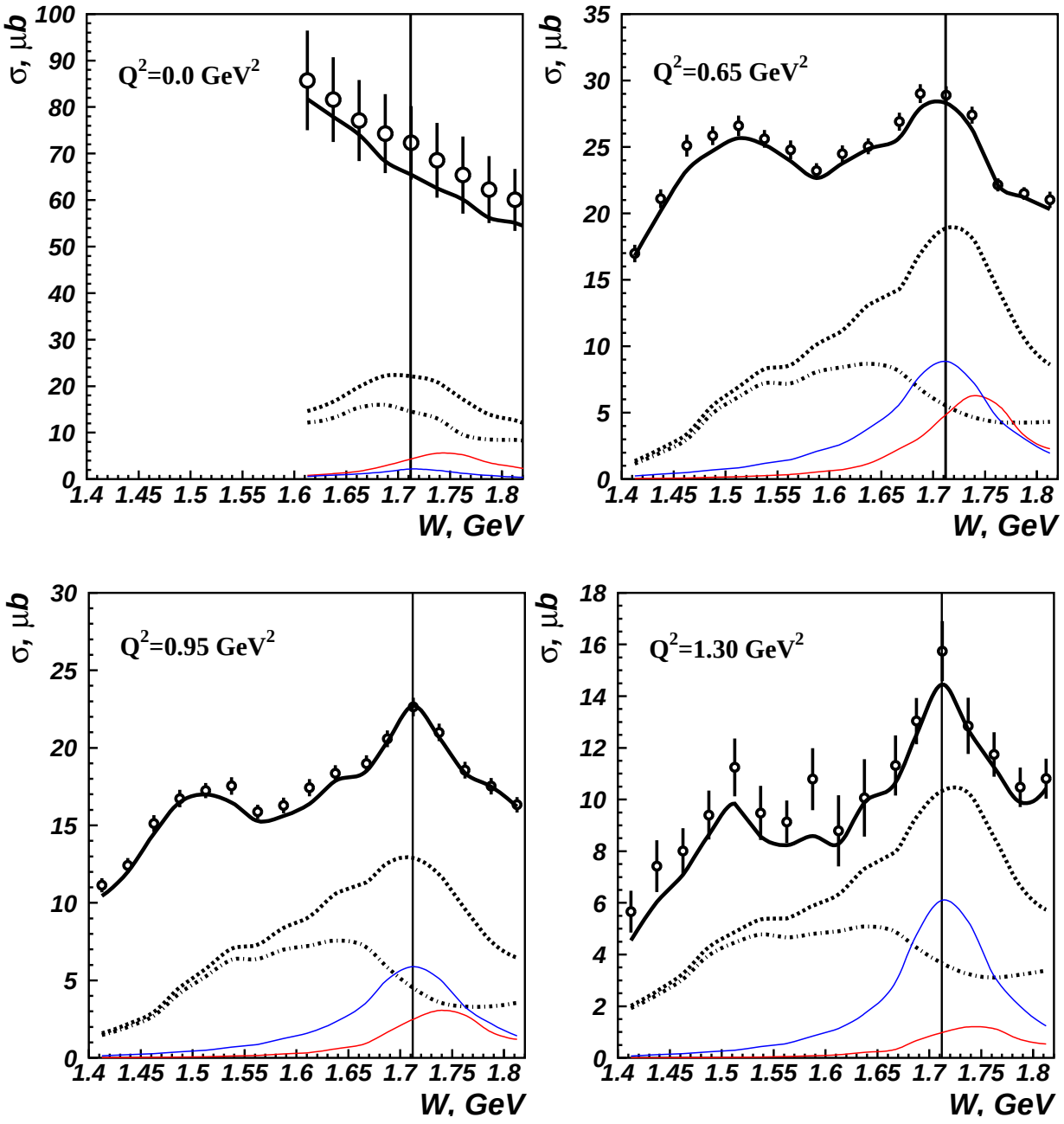

Figure 1: (Color Online) Description of the fully integrated CLAS $\gamma_{r,v}p \to \pi^+\pi^- p'$ photo-/electroproduction cross sections achieved within the JM model [29, 30, 31] (shown by the black solid lines). The error bars include the combined statistical and point-to-point systematic uncertainties for the photoproduction data and only the statistical uncertainties for the electroproduction data. The full resonant contributions are shown by the dashed lines and the dot-dashed lines represent the resonant parts when both the $N(1720)3/2^+$ and $N'(1720)3/2^+$ contributions are taken out. The contributions from the $N(1720)3/2^+$ and $N'(1720)3/2^+$ resonances are shown by the thin red and blue lines, respectively. The vertical lines locate the Breit-Wigner mass of the $N'(1720)3/2^+$ state.

mass range from 1.6–2.0 GeV, their hadronic decays to the $\pi\Delta$ and ρp final states, as well as the electrocouplings of several resonances determined within the JM model are included in the PDG [20].

3. Evidence for the New $N'(1720)3/2^+$ Resonance in the $\pi^+\pi^- p$ Data

The previous studies of $\pi^+\pi^- p$ photo-/electroproduction with CLAS demonstrated a substantial decrease of the relative non-resonant contributions with increasing Q^2 [26, 31]. In the current studies, the resonant structure clearly seen in $\pi^+\pi^- p$ electroproduction at

Table 1: The kinematic grid and the number of data points for the 1-fold $\pi^+\pi^-p$ differential photo-/electroproduction cross sections used in the analysis within the JM model.

Q^2, GeV^2	Number of bins over W, $M_{\pi^-\pi^+}$, $M_{\pi^+p'}$, $M_{\pi^-p'}$ θ_{π^-}, θ_{π^+}, $\theta_{p'}$ $\alpha_{[\pi^-p][\pi^+p']}$, $\alpha_{[\pi^+p][\pi^-p']}$, $\alpha_{[pp'][\pi^-\pi^+]}$	Total number of data points for $\pi^+\pi^-p$
0.0	9, 16, 16, 16, 14, 14, 14, 14, 14, 14	1188
0.65 , 0.95 , 1.30	9, 10, 10, 10, 10, 10, 10, 5, 5, 5	2025

Table 2: $N(1720)3/2^+$ hadronic decay widths and branching fractions into $\pi\Delta$ and ρp determined from independent fits to the data on charged double-pion photo- [26] and electroproduction [23] off protons accounting only for contributions from previously known resonances.

$N(1720)3/2^+$	N^* total width MeV	Branching fraction for decays to $\pi\Delta$	Branching fraction for decays to ρN
electroproduction	126.0 ± 14.0	64% - 100%	<5%
photoproduction	160.0 ± 65.0	14% - 60%	19% - 69%

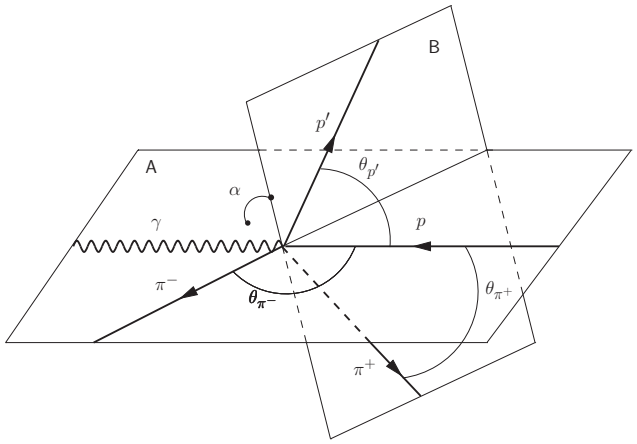

Figure 2: Angular kinematic variables for the reaction $\gamma p \to \pi^+\pi^-p'$ in the CM frame. The variable set with i=π^-, j=π^+, and k=p', includes the angular variables for θ_{π^-} (the polar angle of the π^-) and $\alpha_{[\pi^-p][\pi^+p']}$, which is the angle between the planes A and B, where plane A ($[\pi^-p]$) is defined by the 3-momenta of the π^- and the initial state proton and plane B ($[\pi^+p']$) is defined by the 3-momenta of the π^+ and the final state proton p'. The polar angle $\theta_{p'}$ is relevant for the set with i=p', j=π^+, and k=π^-, while the polar angle θ_{π^+} belongs to the variable set with i=π^+, j=p', and k=π^-.

$W \approx 1.7$ GeV is not visible in the photoproduction data because of the maximal non-resonant contributions at $Q^2 = 0$ GeV^2 (see Fig. 1). On the other hand, the six angular distributions are sensitive to the resonant contributions both in the photo- and electroproduction data. The resonance decays into the $\pi\Delta$ and ρp final states have a substantial impact on the three invariant mass distributions shown in Fig. 3. The Q^2-dependence of the $\pi^+\pi^-p$ photo-/electroproduction amplitudes are defined by the Q^2-evolution of the nucleon resonance photo-/electrocouplings and the real/virtual photon+hadron vertices in the non-resonant mechanisms. However, the resonance masses, as well as their total and partial hadronic decay widths, should remain the same in all Q^2-bins, as was observed in the analyses of all exclusive meson electroproduction data from CLAS [21, 24, 30, 31]. This makes a combined analysis of the $\pi^+\pi^-p$ photo-/electroproduction data of particular importance for establishing the resonances contributing to the $\pi^+\pi^-p$ channel.

The analyses of the CLAS $\pi^+\pi^-p$ photo- [26] and electroproduction [23] data were carried out within the recent version of the JM model in the W-range from 1.6 – 1.8 GeV and for Q^2 from 0.0 – 1.5 GeV^2 with the goal to establish the resonances contributing in the third resonance region. For the $N(1440)1/2^+$, $N(1520)3/2^-$, and $\Delta(1620)1/2^-$ resonances, the initial values of their $\pi\Delta$ and ρp decay widths were taken from analyses of the CLAS $\pi^+\pi^-p$ electroproduction data [30, 31], while for the other resonances we used the total hadronic decay widths from the PDG [20] and the branching fractions for their decays into the $\pi\Delta$ and ρp final states from Ref. [32]. The initial values of the resonance photo-/electrocouplings were taken from the parameterization in Ref. [33] of the available CLAS/world data results detailed in Ref. [34]. The starting values of the photo-/electrocouplings and the decay widths into the $\pi\Delta$ and ρp final states for the new $N'(1720)3/2^+$ resonance were taken from Refs. [23, 26].

In the data fit we simultaneously varied the resonance

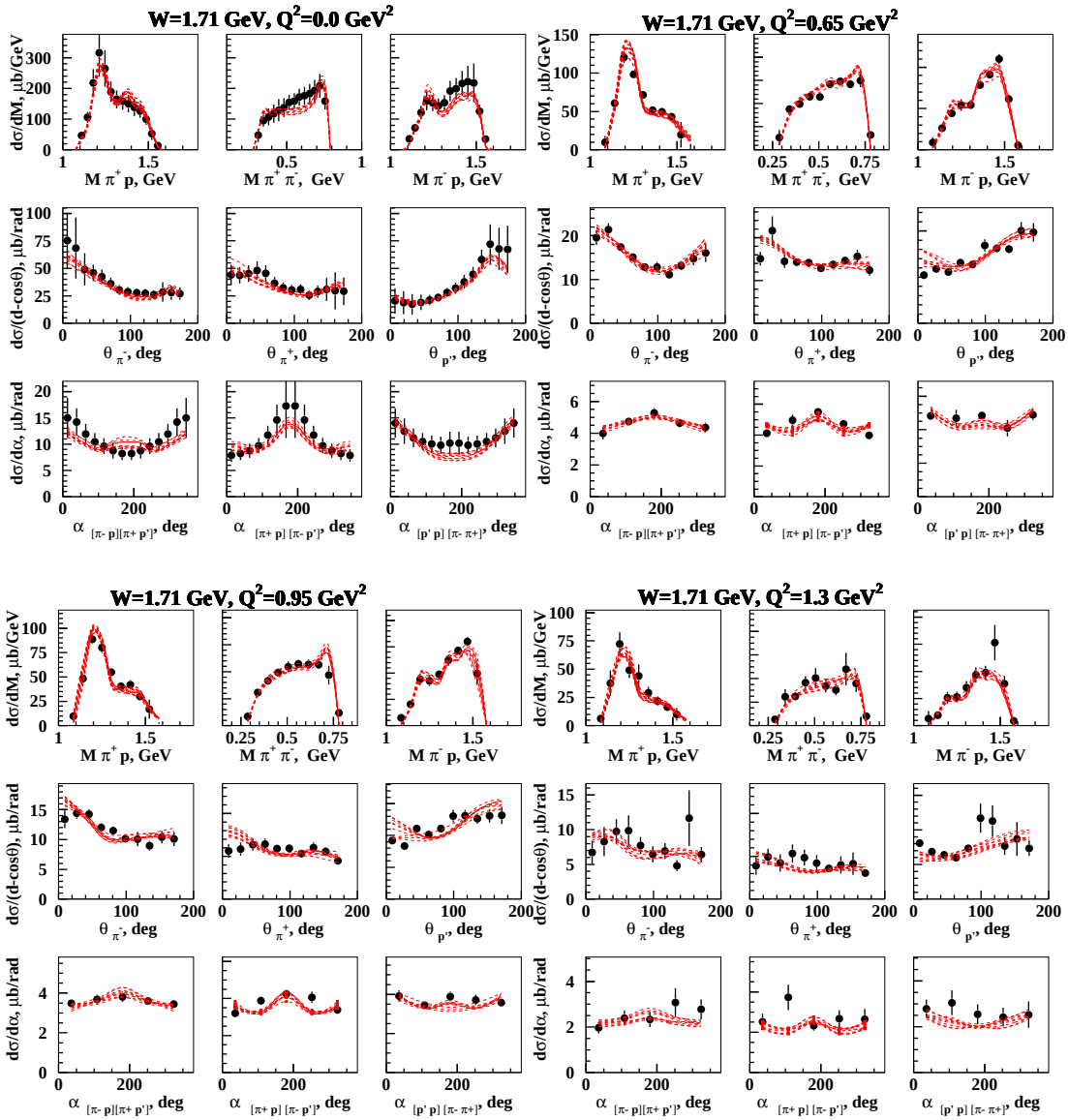

Figure 3: (Color Online) Representative examples for the description of the $\gamma_{r,v}p \to \pi^+\pi^-p'$ nine 1-fold differential cross sections achieved within the JM model [26, 30, 31] for photo- and electroproduction (red curves) in comparison with the data [23, 26]. The error bars include the combined statistical and point-to-point systematic uncertainties for the photoproduction data and only the statistical uncertainties for the electroproduction data. The group of curves on each plot correspond to the computed cross sections selected in the data fit with $\chi^2/d.p. < \chi^2/d.p.^{max}$ (see Section 3 for details). Fits with Q^2-independent masses, and total and partial decay widths into the $\pi\Delta$ and ρp final states, for all contributing resonances become possible only after the implementation of the new $N'(1720)3/2^+$ state.

photo-/electrocouplings, the $\pi\Delta$ and ρp decay widths, and the parameters of the non-resonant amplitudes described in Refs. [26, 30, 31]. Q^2-independent hadronic decay widths for all resonances were imposed in the fit. The parameters of the resonant and non-resonant mechanisms of the JM model were sampled around their initial values, employing unrestricted normal distributions with a width (σ) of 30% of their initial values. In this way, the JM model provided a description of the observables within their uncertainties for most of the data points. For each trial set of the fit parameters, we computed the nine 1-fold differential $\pi^+\pi^-p$ cross sections and estimated the χ^2/dp ($dp \equiv$ data point) values in point-by-point comparisons. We selected the computed cross sections from the data fit within the range $\chi^2/dp < \chi^2/dp^{max}$, where χ^2/dp^{max} was determined so that the computed cross sections were within the data uncertainties for most data points. The mean values and RMS widths for the resonance parameters obtained from the fit were used as estimates of their central values and their corresponding uncertainties.

Analyses of the $\pi^+\pi^-p$ photo- and electroproduction data were carried out independently. The resonance photo-/electrocouplings and the total, $\pi\Delta$, and ρp decay widths were inferred from the fits over W from 1.6

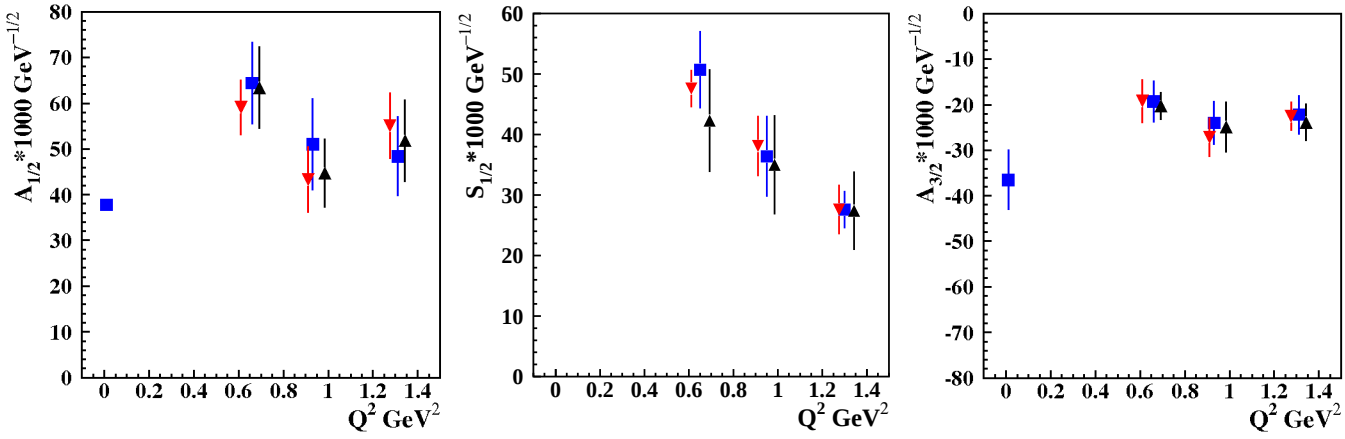

Figure 4: (Color Online) Photo-/electrocouplings of the new $N'(1720)3/2^+$ state determined from independent analyses of three overlapping W-intervals: a) from 1.61 – 1.71 GeV (red triangles), b) from 1.66 – 1.76 GeV (blue squares), and c) from 1.71 – 1.81 GeV (black triangles). The blue squares at the photon point show the results of the CLAS charged double-pion photoproduction data analysis [26].

– 2.0 GeV for the photoproduction data, and over W from 1.6 – 1.8 GeV and Q^2 from 0.5 – 1.5 GeV^2 for the electroproduction data. In the evaluation of χ^2/dp for the electroproduction data, only the statistical uncertainties were taken into account, while for the photoproduction data, the combined contribution from the statistical and point-to-point systematic uncertainties was employed since the systematic uncertainties dominate the accuracy of the photoproduction data. Parity conservation imposes the requirement of equal values of the $\frac{d\sigma}{d\alpha_i}$ $(i = \pi^+, \pi^-, p')$ cross sections at the angles α_i and $2\pi - \alpha_i$. This symmetry requirement was accounted for in the computation of these cross sections within the JM model. The departure of the data points from this requirement, seen only in the Q^2=1.3 GeV^2 bin, was taken into account in the evaluation of χ^2/dp.

A successful description of the angular θ_i $(i = \pi^+, \pi^-, p')$ distributions at $W \approx 1.7$ GeV requires substantial resonant contributions with $J^P = 3/2^+$ spin-parity. This is consistent with the results from previous studies [23]. The essential role of the $J^P = 3/2^+$ spin-parity excited nucleon states in the generation of the resonant contributions in the third resonance region can be seen in Fig. 1, where the resonant contributions in the fully integrated $\pi^+\pi^- p$ photo-/electroproduction cross sections are presented with all relevant resonances included and when the contributions from the $N(1720)3/2^+$ and $N'(1720)3/2^+$ resonances are taken out.

We performed two different fits using:

- the contributions from only well-established resonances listed in Refs. [26, 31], including the $N(1700)3/2^-$ and $N(1720)3/2^+$ states (fit A);
- the fit A assumptions also adding a new $N'(1720)3/2^+$ resonance with mass, total, $\pi\Delta$, and ρp decay widths, and photo-/electrocouplings fit to the data (fit B).

Both fits result in good descriptions of the CLAS data with a comparable quality for photo- and electroproduction. Representative examples of the description of the nine 1-fold differential cross sections with fit B are shown in Fig. 3, where the cross sections from the fits within the range $\chi^2/dp < \chi^2/dp^{max}$ are shown by the family of curves overlaid on each plot.

Note that the decay widths of the well-known $N(1720)3/2^+$ resonance into the $\pi\Delta$ and ρp final states depend considerably on the implementation of the new $N'(1720)3/2^+$ state. Accounting for only the well-known resonances results in contradictory values for the $N(1720)3/2^+$ decays into the ρp final state inferred either from the independent photo- or electroproduction data fits with more than a factor of four difference (see Table 2). This makes it impossible to describe both the $\pi^+\pi^- p$ photo- and electroproduction cross sections with Q^2-independent resonance masses, as well as total and partial hadronic decay widths, accounting for only the well-known resonances.

After implementation of the new $N^{'}(1720)3/2^+$ resonance, a successful description of all nine 1-fold differential $\gamma_{r,v}p \to \pi^+\pi^- p$ photo-/electroproduction cross sections has been achieved. The total, $\pi\Delta$, and ρp hadronic decay widths of all resonances in the third resonance region as inferred from the fits at different Q^2-bins remain Q^2-independent (see Table 3) over the entire range of Q^2 up to 1.5 GeV^2 that is covered by the measurements [23, 26]. This supports the existence of the new $N'(1720)3/2^+$ resonance. Indeed, if the implementation of this (or any) new baryon state was unphysical, then it would not be possible to reproduce the $\pi^+\pi^- p$ photo-/electroproduction data in a wide Q^2-range with Q^2-independent decay widths because of the evolution of the non-resonant contributions with Q^2 observed in the $\pi^+\pi^- p$ electroproduction data [31].

The electrocouplings of the new $N'(1720)3/2^+$ resonance were determined in independent data fits for Q^2 in the range from 0.5 – 1.5 GeV^2 within the three overlapping

Table 3: Hadronic decays into the $\pi\Delta$ and ρp final states of the resonances in the third resonance region with major decays to the $\pi^+\pi^- p$ final state determined from the fits to the data on charged double-pion photo- [26] and electroproduction [23] implementing a new $N'(1720)3/2^+$ baryon state.

Resonance states	N^* total width MeV	Branching fraction for decays to $\pi\Delta$	Branching fraction for decays to ρp
$\Delta(1700)3/2^-$			
electroproduction	288.0 ± 14.0	77 - 95%	3 - 5%
photoproduction	298.0 ± 12.0	78 - 93%	3 - 6%
$N(1720)3/2^+$			
electroproduction	116.0 ± 7.0	39 - 55%	23 - 49%
photoproduction	112.0 ± 8.0	38 - 53%	31 - 46%
$N'(1720)3/2^+$			
electroproduction	119.0 ± 6.0	47 - 64%	3 - 10%
photoproduction	120.0 ± 6.0	46 - 62%	4 - 13%

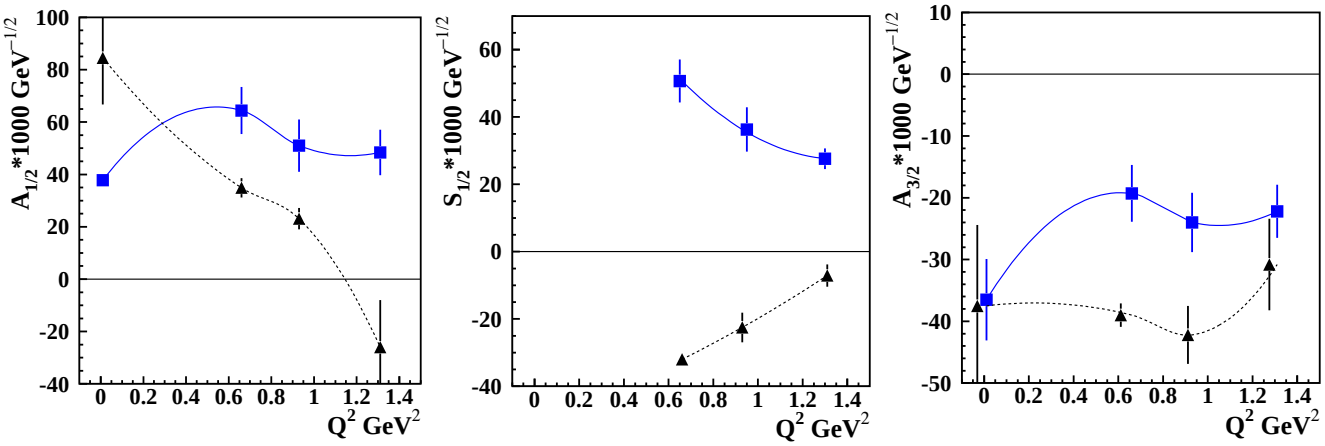

Figure 5: (Color Online) Comparison between the photo- and electrocouplings of the $N(1720)3/2^+$ (black triangles connected by dashed lines) and the new $N'(1720)3/2^+$ (blue squares connected by solid lines) obtained from the CLAS $\pi^+\pi^- p$ photo- and electroproduction data [23, 26].

W-intervals: 1.61 – 1.71 GeV, 1.66 – 1.76 GeV, and 1.71 – 1.81 GeV (see Fig. 4). The non-resonant contributions in the three W-intervals are different, while the extracted $N'(1720)3/2^+$ electrocouplings agree within the uncertainties, which underlines the credible extraction of the electrocouplings. Furthermore, the $N'(1720)3/2^+$ mass, as well as the total and partial decay widths into the $\pi\Delta$ and ρp final states obtained from the fits in the three W-intervals, are also consistent, which further supports the existence of this new state.

Comparisons between the photo-/electroexcitation amplitudes of the $N(1720)3/2^+$ state and the new $N'(1720)3/2^+$ state determined from the CLAS $\pi^+\pi^- p$ photo-/electroproduction data [23, 26] are shown in Fig. 5. The transverse $A_{1/2}$ amplitude of the $N(1720)3/2^+$ resonance decreases with Q^2 more rapidly than for the new $N'(1720)3/2^+$ state.

The contributions of the $N(1720)3/2^+$ and $N'(1720)3/2^+$ resonances to the fully integrated $\pi^+\pi^- p$ photo-/electroproduction cross sections are shown in Fig. 1. As Q^2 increases the contributions from the $N'(1720)3/2^+$ become more pronounced relative to the $N(1720)3/2^+$. Both resonances are more visible in the electroproduction data compared to photoproduction. The sizable increase of the non-resonant contributions seen in the $\pi^+\pi^- p$ photoproduction data reduces the relative contributions from these resonances.

Nevertheless, the combined studies of the $\pi^+\pi^- p$ photo-/electroproduction data are critical in order to validate the contributions from both the $N(1720)3/2^+$ and $N'(1720)3/2^+$ resonances. In the analyzed data set, it is only at the photon point that the contribution from the $N(1720)3/2^+$ is larger than that of the new $N'(1720)3/2^+$. The branching fraction range for the $N(1720)3/2^+$ decay from the photoproduction data into the ρp final state, >19%, is imposed by the behavior of the high-mass part of the $\pi^+\pi^-$ mass distribution. This established range makes it impossible to simultaneously describe the $\pi^+ p$ and $\pi^+\pi^-$ invariant mass distributions in the electroproduction data assuming only the contribution from the $N(1720)3/2^+$ resonance. This includes the pronounced Δ^{++} peaks seen in the $\pi^+ p$ mass distributions and the absence of the ρ

Table 4: Masses and hadronic decay widths of the $N(1720)3/2^+$ and $N'(1720)3/2^+$ resonances to the $\pi\Delta$ and ρp final states determined from the CLAS data on charged double-pion photo- and electroproduction off protons [23, 26].

Resonance states	Mass, GeV	N^* total width, MeV	Branching fraction for decays to $\pi\Delta$	Branching fraction for decays to ρp
$N(1720)3/2^+$	1.743-1.753	114 ± 6	38-53%	31-46%
$N'(1720)3/2^+$	1.715-1.735	120 ± 6	47-62%	4-10%

peak in the $\pi^+\pi^-$ mass distributions (see Fig. 3). In order to reproduce the Δ^{++} peaks seen in the π^+p mass distributions without including the $N'(1720)3/2^+$ state, the $N(1720)3/2^+$ decay widths to the ρp final state would have to be more than a factor of four smaller in electroproduction compared with the values established in photoproduction. When a new $N'(1720)3/2^+$ resonance is implemented, the Δ^{++} peaks in the electroproduction data in the π^+p mass distributions can be well described by the contributions from the new $N'(1720)3/2^+$ state, which has only minor (<13%) hadronic decays to the ρp final state. A rapid decrease of the $A_{1/2}$ electrocoupling of the $N(1720)3/2^+$ with Q^2 (see Fig. 5) allows for the description of the $\pi^+\pi^-$ invariant mass distributions both in the photo- and electroproduction data, reproducing the high-mass part without the ρ peak in the electroproduction reaction.

The masses, total decay widths, and branching fractions for the decays of these resonances into $\pi\Delta$ and ρp are listed in Table 4. The new $N'(1720)3/2^+$ decays mostly into the $\pi\Delta$ final state, while the $N(1720)3/2^+$ decay widths into the $\pi\Delta$ and ρp final states are comparable. The contributions from the $N(1720)3/2^+$ and the new $N'(1720)3/2^+$ resonances are well separated in the $\pi^+\pi^-p$ photo-/electroproduction data analyses despite the close masses and the same spin-parity of these states. Different patterns for the decays into the $\pi\Delta$ and ρp final states and the different Q^2-evolution of the resonance electrocouplings allow us to disentangle their contributions. These differences can be seen in the combined studies of $\pi^+\pi^-p$ photo- and electroproduction, but they are elusive in the previous studies of the two-body meson-baryon channels, as well as the $\pi\pi N$ channels limited to photoproduction data only. Note that a global coupled-channel analysis of the exclusive meson photo- and hadroproduction data [27] has revealed evidence for two nucleon resonances of $J^P = 3/2^+$ and I=1/2 for W from 1.7 – 1.8 GeV, supporting our observation of both the $N(1720)3/2^+$ and the new $N'(1720)3/2^+$ states.

4. Shedding Light on the Nature of New Baryon States

The discovery of several new resonances in the global multi-channel analysis of exclusive meson photoproduction data [15] is consistent with the pattern from approximate SU(6) spin-flavor symmetry in the generation of the N^* spectrum. Most of the states predicted in the $[70, 2^+]$ multiplet have been observed. Two of them, the $N(1880)1/2^+$ and $N(1900)3/2^+$ with a 4-star status, and three others with a lower rating, are included in the PDG [20]. However, one of the $[70, 2^+]$ multiplet states of $J^P = 3/2^+$ and isospin I=1/2 [9] remains elusive. Is it possible that the new $N'(1720)3/2^+$ resonance established in our analyses is this expected state? In order to obtain an answer, we have estimated the mass of this state from the SU(6) symmetry pattern for the masses of the nucleon resonances in the $[70, 2^+]$ and $[70, 1^-]$ multiplets. There are two resonances in the $[70, 2^+]$ multiplet with a total quark spin S_q=1/2: the still unknown state of $J^P = 3/2^+$, isospin I=1/2 and the $N(1860)5/2^+$. Four other states of S_q=3/2 are the $N(1880)1/2^+$, $N(1900)3/2^+$, $N(2000)5/2^+$, and $N(1900)7/2^+$ resonances. Their average mass is equal to 1.955 GeV. We assume that the difference between the average mass values for the resonances of S_q=1/2 and S_q=3/2, $\Delta M(S_{3/2} - S_{1/2})$, in the $[70, 2^+]$ multiplet is the same as in the $[70, 1^-]$. For the $[70, 1^-]$ multiplet, $\Delta M(S_{3/2} - S_{1/2}) = 0.16$ GeV is obtained by averaging the differences between the masses of the resonances $N(1650)1/2^-$, $N(1535)1/2^-$ and $N(1700)3/2^-$, $N(1520)3/2^-$ with S_q=1/2 and S_q=3/2. Hence, the average mass for the resonances of S_q=1/2, $M^{av}_{S=1/2}$, in the $[70, 2^+]$ multiplet can be estimated as:

$$\begin{aligned} M^{av}_{S=1/2} &= M^{av}_{S=3/2} - \Delta M(S_{3/2} - S_{1/2}) \\ &= 1.955\,\text{GeV} - 0.16\,\text{GeV} = 1.795\,\text{GeV}. \end{aligned} \quad (1)$$

The mass of the $N(1880)1/2^+$ state is smaller by ΔM=0.075 GeV than $M^{av}_{S=3/2}$=1.955 GeV for the four resonances of $S_q = 3/2$ in the $[70, 2^+]$ multiplet. Assuming the same ΔM for the S_q=1/2 doublet of resonances in the $[70, 2^+]$ multiplet, the mass of the lightest resonance of S_q=1/2, $M_{3/2^+}$, can be evaluated as:

$$\begin{aligned} M_{3/2^+} &= M^{av}_{S=1/2} - \Delta M \\ &= 1.795\,\text{GeV} - 0.075\,\text{GeV} = 1.72\,\text{GeV}. \end{aligned} \quad (2)$$

The estimated value of $M_{3/2^+}$ is in good agreement with the mass of the new $N'(1720)3/2^+$ resonance from our analysis (see Table 4), which makes plausible the assignment of the state as the lightest resonance in the $[70, 2^+]$ multiplet of $J^P = 3/2^+$ and isospin I=1/2.

A variety of quark models predict two close resonances of $J^P = 3/2^+$ and I=1/2, consistent with those seen in

our analysis. The interacting quark-diquark [28] and the hypercentral constituent quark model [7] predict two states of $J^P = 3/2^+$ and I=1/2 in the mass range from 1.7 – 1.8 GeV. The conceptually different chiral quark-soliton model [8] with parameters fit to the baryon masses in the octet and decuplet predicts a resonance of $J^P = 3/2^+$, I=1/2 in addition to the $N(1720)3/2^+$ as a member of the 27-SU(3)-baryon multiplet. The computed mass of this state of 1718.6 ± 7.4 MeV is consistent with the mass of the new $N'(1720)3/2^+$ state (see Table 4). The results on the Q^2-evolution of the $N(1720)3/2^+$ and $N'(1720)3/2^+$ resonance electrocouplings have become available from our analysis for the first time (see Fig. 5). Confronting our findings with the quark model expectations will shed light on the missing resonance nature, elucidating the peculiar features of strong QCD that have made these states elusive for such a long time.

5. Summary

The analysis of the CLAS $\pi^+\pi^-p$ photo-/electroproduction data [23, 26] has been carried out for W from 1.6 – 1.8 GeV and for Q^2 from 0 – 1.5 GeV^2 with the goal to establish the nucleon resonances in the third resonance region contributing to this channel. Accounting for only the well-established resonances results in more than a factor of four difference for the decay branching fractions of the $N(1720)3/2^+$ resonance into the ρp final state as inferred from independent fits of the $\pi^+\pi^-p$ photo-/electroproduction data (see Table 2). This contradiction makes it impossible to describe both the photo- and electroproduction data unless the contributions from a still unobserved resonance are added.

After implementation of the $N'(1720)3/2^+$ resonance with photo-/electrocouplings, mass, and decay widths fit to the CLAS data [23, 26] (see Table 4 and Fig. 5), a successful description of the $\pi^+\pi^-p$ photo-/electroproduction data is achieved with Q^2-independent masses and total and partial decay widths into the $\pi\Delta$ and ρp final states of all contributing resonances in the third resonance region. Moreover, the photo-/electrocouplings and hadronic decay widths of all contributing resonances coincide within their uncertainties determined from the independent fits in three overlapping W-intervals (see Fig. 4). The evolution with Q^2 of the non-resonant contributions to $\pi^+\pi^-p$ electroproduction observed in the previous CLAS data analysis [31] makes it unlikely that the implementation of the $N'(1720)3/2^+$ resonance can serve as an effective way to describe the non-resonant contributions beyond the scope of the JM model and, therefore, these results support the existence of the new $N'(1720)3/2^+$ state. A manifestation of the new $N'(1720)3/2^+$ baryon state was also found in an independent global coupled-channel analysis of the exclusive meson photo- and hadroproduction data [27], which also revealed evidence for two nearby resonances of $J^P = 3/2^+$ and I=1/2 for W from 1.7 – 1.8 GeV.

The first results on the Q^2-evolution of the photo-/electroexcitation amplitudes of the missing baryon states have become available for the $N'(1720)3/2^+$. Confronting these results with the quark model predictions will shed light on the nature of the missing resonances. In the future, the observation of the new $N'(1720)3/2^+$ state will be also checked in the analysis of the recent high quality $\pi^+\pi^-p$ electroproduction data from CLAS [25, 35, 36] in the Q^2 range from 0.4 – 5.0 GeV^2. These data will provide the TT and LT interference structure functions [36] allowing for improvement in the evaluation of the resonance electrocouplings.

Additional data on $\pi^+\pi^-p$ electroproduction at $Q^2 <$ 0.4 GeV^2 are needed in order to explore the range of photon virtualities in Fig. 1 where the transition occurs from $N(1720)3/2^+$ dominance in photoproduction to $N'(1720)3/2^+$ dominance in electroproduction. The measurement of beam, target, and beam-target asymmetries will be very helpful for the resonance electrocoupling extraction, in particular at $Q^2 <$ 0.4 GeV^2 where the non-resonant contributions become increasingly important as Q^2 goes to zero. Our results on the mass, total decay width, and electrocouplings of the $N'(1720)3/2^+$ will guide the search for the manifestation of this state in other meson electroproduction channels: KY, ωp, ϕp, $\pi\eta N$. The studies of exclusive $\pi\pi N$ hadroproduction planned at JPARC [37] will allow for the exploration of the manifestation of the $N'(1720)3/2^+$ resonance in such reactions and to independently establish from hadroproduction data the $N(1720)3/2^+$ and $N'(1720)3/2^+$ decay widths to the $\pi\Delta$ and ρp final states.

6. Acknowledgments

We express our gratitude for valuable theoretical support by I.G. Aznauryan, T-S.H. Lee, C.D. Roberts, E. Santopinto, and A.P. Szczepaniak. We would like to acknowledge the outstanding efforts of the staff of the Accelerator and the Physics Divisions at Jefferson Lab that made the experiments possible. This work was supported in part by the U.S. Department of Energy, the National Science Foundation, the University of Connecticut, Ohio University, the Skobeltsyn Institute of Nuclear Physics, the Physics Department at Moscow State University, and the University of South Carolina. This material is based upon work supported by the U.S. Department of Energy, Office of Science, Office of Nuclear Physics under contract DE-AC05-06OR23177. The U.S. Government retains a non-exclusive, paid-up, irrevocable, world-wide license to publish or reproduce this manuscript for U.S. Government purposes.

References

[1] V.D. Burkert, Few Body Syst. **57**, 873 (2016).
[2] V. Crede and W. Roberts, Rep. Prog. Phys. **76**, 076301 (2013).

[3] D.G. Ireland, E. Pasyuk, and I. Strakovsky, Prog. Part. Nucl. Phys., **111** 103752 (2020).
[4] E. Klempt *et al.*, EPJ Web Conf. **134**, 02002 (2017).
[5] R. Beck *et al.*, EPJ Web Conf. **134**, 02001 (2017).
[6] S. Capstick and W. Roberts, Prog. Part. Nucl. Phys. **45**, S241 (2000).
[7] M.M. Giannini and E. Santopinto, Chin. J. Phys. **53**, 020301 (2015).
[8] G.-S. Yang and H.-C. Kim, PTEP, 093D01 (2019).
[9] E. Klempt and B. Ch. Metsch, Eur. Phys. J. A**48**, 127 (2012).
[10] J.J. Dudek and R.G. Edwards, Phys. Rev. D **85**, 054016 (2012).
[11] H.L.L. Roberts *et al.*, Few Body Syst. **51**, 1 (2011).
[12] Chen Chen *et al.*, Phys. Rev. D **100**, 054016 (2019).
[13] A. Bazavov *et al.*, Phys. Rev. Lett. **113**, 072001 (2014).
[14] S. Capstick, Nucl. Phys. Proc. Suppl. **45**, 241 (2000).
[15] A.V. Anisovich *et al.*, Phys. Rev. Lett. **119**, 062004 (2017).
[16] R.K. Bradford *et al. (CLAS Collaboration)*, Phys. Rev. C **73**, 035202 (2006).
[17] R.K. Bradford *et al. (CLAS Collaboration)*, Phys. Rev. C **75**, 035205 (2007).
[18] M.E. McCracken *et al. (CLAS Collaboration)*, Phys. Rev. C **81**, 025201 (2010).
[19] B. Dey *et al. (CLAS Collaboration)*, Phys. Rev. C **82**, 025202 (2010).
[20] M. Tanabashi *et al. (Particle Data Group)*, Phys. Rev. D **98**, 03001 (2018).
[21] V.I. Mokeev, arXiv:1909.08746 [nucl-ex].
[22] V.I. Mokeev *et al.*, EPJ Web Conf. **113**, 01013 (2016).
[23] M. Ripani *et al. (CLAS Collaboration)*, Phys. Rev. Lett. **91**, 022002 (2003).
[24] I.G. Aznauryan and V. D. Burkert, Prog. Nucl. Part. Phys. **67**, 1 (2012).
[25] E.L. Isupov *et al. (CLAS Collaboration)*, Phys. Rev. C **96**, 025209 (2017).
[26] E.N. Golovatch *et al. (CLAS Collaboration)*, Phys. Lett. B **788**, 371 (2019).
[27] H. Kamano *et al.*, Phys. Rev. **C 88**, 035209 (2013).
[28] E. Santopinto and J. Ferretti, Phys. Rev. **C 92**, 025202 (2015).
[29] V.I. Mokeev *et al.*, Phys. Rev. **C 80**, 045212 (2009).
[30] V.I. Mokeev *et al. (CLAS Collaboration)*, Phys. Rev. **C 86**, 035203 (2012).
[31] V.I. Mokeev *et al.*, Phys. Rev. C **93**, 054016 (2016).
[32] D.M. Manley and E.M. Salesky, Phys. Rev. D **45**, 4002 (1992).
[33] A.N. Hiller Blin *et al.*, Phys. Rev. **C 100**, 035201 (2019).
[34] Nucleon Resonance Photo-/Electrocouplings Determined from Analyses of Experimental Data on Exclusive Meson Electroproduction off Protons, `https://userweb.jlab.org/~mokeev/resonance_electrocouplings/`
[35] G.V. Fedotov *et al. (CLAS Collaboration)*, Phys. Rev. **C 98**, 025203 (2018).
[36] A. Trivedi, Few Body Syst. **60**, 45 (2019).
[37] K.H. Hicks and H. Sako, J-PARC experiment E45, "3-Body Hadronic Reactions for New Aspects of Baryon Spectroscopy", 2012, http://j-parc.jp/researcher/Hadron/en/Proposal_e.html